Computer-Aided Design, Synthesis, and Anti-HIV-1 Activity in Vitro of 2-Alkylamino-6-[1-(2,6-difluorophenyl)alkyl]-3,4-dihydro-5-alkylpyrimidin-4(3*H*)-ones as Novel Potent Non-Nucleoside Reverse Transcriptase Inhibitors, Also Active Against the Y181C Variant

Rino Ragno,[†] Antonello Mai,[§] Gianluca Sbardella,[#] Marino Artico,*[,§] Silvio Massa,[¶] Chiara Musiu,[⊥] Massimo Mura,[⊥] Flavia Marturana,[⊥] Alessandra Cadeddu,[⊥] and Paolo La Colla*[,‡]

Dipartimento di Studi di Chimica e Tecnologie delle Sostanze Biologicamente Attive, Università degli Studi di Roma "La Sapienza", P.le A. Moro 5, I-00185 Roma, Italy, Istituto Pasteur-Fondazione Cenci Bolognetti, Dipartimento di Studi Farmaceutici, Università degli Studi di Roma "La Sapienza", P.le A. Moro 5, I-00185 Roma, Italy, Dipartimento di Scienze Farmaceutiche, Università degli Studi di Salerno, Via Ponte Don Melillo, I-84084 Fisciano (SA), Italy, Dipartimento Farmaco Chimico Tecnologico, Università degli Studi di Siena, via Aldo Moro, I-53100 Siena, Italy, Cooperative Laboratories Idenix, Università degli Studi di Cagliari, Cittadella Universitaria SS 554, I-09042 Monserrato (Cagliari), Italy, and Dipartimento di Scienze e Tecnologie Biomediche, Università degli Studi di Cagliari, Cittadella Universitaria SS 554, I-09042 Monserrato (Cagliari), Italy

Received August 4, 2003

Dihydro-alkoxy-benzyl-oxopyrimidines (DABOs) are a family of potent NNRTIs developed in the past decade. Attempts to improve their potency and selectivity led to thio-DABOs (*S*-DABOs), DATNOs, and difluoro-thio-DABOs (F_2-*S*-DABOs). More recently, we reported the synthesis and molecular modeling studies of a novel conformationally constrained subtype of the *S*-DABO series characterized by the presence of substituents on the methylene linkage connecting the pyrimidine ring to the aryl moiety (Mai, A., et al. *J. Med. Chem.* **2001**, *44*, 2544−2554). Now we report the computer-aided design, synthesis, and biological evaluation of four new DABO prototypes (5-alkyl-2-cyclopentylamino-6-[1-(2,6-difluorophenyl)alkyl]-3,4-dihydropyrimidin-4(3*H*)-ones, F_2-*NH*-DABOs) in which the sulfur atom of the related F_2-*S*-DABOs is replaced by an amino group. For these studies, we used as a reference model the cocrystallized MKC-442/RT complex. Docking studies with Autodock of the newly designed F_2-*NH*-DABOs on the ligand-derived RT confirmed the findings previously described for the F_2-*S*-DABOs. The F_2-*NH*-DABO binding mode resembles that reported for F_2-*S*-DABOs, with the difference that the NH moiety at the C-2 position represents a new anchor site for ligand/enzyme complexation. The predicted inhibition constant (K_i) values by the internal scoring function of Autodock, and the predicted IC_{50} values by the application of a VALIDATE II/HIV-RT model strongly suggested the synthesis of the designed amino-DABOs. F_2-*NH*-DABOs were shown to be highly active in both anti-RT and anti-HIV biological assays with IC_{50} and EC_{50} comparable with that of the reference compound MKC-442. Interestingly, 2-cyclopentylamino-6-[1-(2,6-difluorophenyl)ethyl]-3,4-dihydro-5-methyl pyrimidin-4(3*H*)-one (**9d**) was active against the Y181C HIV-1 mutant strain at submicromolar concentration, with a resistance value similar to that of efavirenz, the last FDA-approved NNRTI for AIDS therapy, and 2-fold lower than that of its 2-cyclopentylthio counterpart **8d**. The introduction in **9d** of a new anchor point (pyrimidine C-2 NH group), with the formation of a new hydrogen bond with Lys101, could compensate for the lack of positive hydrophobic ligand/NNBP interactions due to the Tyr181 to Cys181 mutation.

Introduction

The reverse transcriptase (RT) of human immunodeficiency virus (HIV) is an attractive target for development of selective inhibitors. It is a multifunctional enzyme critical to the retroviral life cycle with no counterpart in eukaryotic systems. Currently, two functionally distinct classes of HIV RT inhibitors (nucleoside and non-nucleoside) have been discovered and are being used clinically. Nucleoside inhibitors of RT (NRTIs), which include AZT, ddI, ddC, d4T, 3TC, abacavir, and tenofovir disoproxil fumarate, act as DNA chain-terminating analogues of the natural deoxynucleoside triphosphates (dNTPs). They are equally active against HIV-1 and HIV-2 RT, and they can also be incorporated into cellular DNA by host DNA polymerases causing severe adverse reactions. Moreover, following long-term administration their effectiveness is limited by the emergence of drug-resistant mutants.[1,2] On the other hand, non-nucleoside RT inhibitors (NNRTIs) are highly specific for HIV-1 and include more than 30 structurally

* To whom correspondence should be sent. M.A.: tel and fax: +39064462731; e-mail: marino.artico@uniroma1.it. P.L.C:-tel +390706754147; fax +390706754210; e-mail: placolla@unica.it.
[†] Dipartimento di Studi di Chimica e Tecnologie delle Sostanze Biologicamente Attive, Università degli Studi di Roma "La Sapienza".
[§] Dipartimento di Studi Farmaceutici, Università degli Studi di Roma "La Sapienza".
[#] Università degli Studi di Salerno.
[¶] Università degli Studi di Siena.
[⊥] Cooperative Laboratories Idenix − Università di Cagliari.
[‡] Università degli Studi di Cagliari.

10.1021/jm0309856 CCC: $27.50
Published on Web 01/08/2004

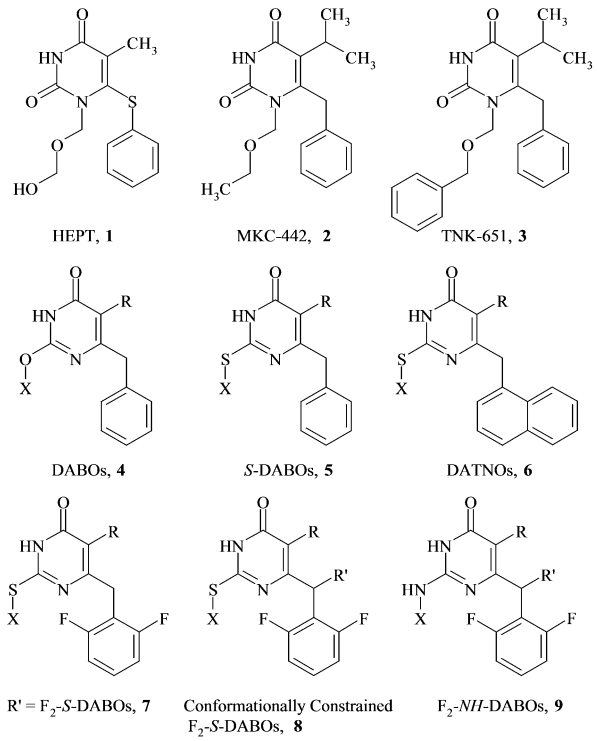

Figure 1. Structures of HEPT, DABOs, and related derivatives.

different classes of molecules. Among them, nevirapine, delavirdine, efavirenz, HEPT (**1**) (Figure 1), TIBO, BHAP, TSAO, α-APA, PETT, oxathiin carboxanilide, and DABO are the most representative.[3−5] Although these agents are highly potent inhibitors of HIV-1 RT, with generally low toxicity and favorable pharmacokinetic properties, their clinical use is limited by the rapid selection of mutants that show cross-resistance to other members of the class.[6,7] In the NNRTI field, therefore, interest is focused on compounds that are highly potent against wild type HIV-1 and demonstrate the capability of inhibiting clinically resistant mutants.[8−11]

Studies carried out on crystal structures of different RT/NNRTI complexes suggest that NNRTIs share a common mode of action. They bind at a single site (non-nucleoside binding pocket, NNBP) that is close to, but distinct from, the polymerase catalytic site.[12−18] Upon binding, NNRTIs distort the polymerase active site and alter the conformation of Tyr181, Tyr183, and Tyr188 residues with respect to that of unliganded RT, leading to conformations virtually indistinguishable from those present in the inactive p51 subunit of the enzyme.[12,14−18]

Interestingly, some potent HIV-1 inhibitors (Table 1) such as nevirapine, TIBO, and two HEPT-like compounds (MKC-442, **2** and TNK-651, **3**) (Figure 1) force Tyr181 into the p51-like conformation ("trigger" action) with their *N*-cyclopropyl, 5-(*S*)-methyl, and C-5-*iso*-propyl groups, respectively.[17,19] All of the above groups are sterically equivalent and clash severely with Tyr181, generating the "trigger" action.[14,16,17]

On the contrary, HEPT does not produce any "trigger effect". Its weak anti-HIV-1 activity ($IC_{50} = 17\ \mu M$) can be explained by taking into account that the C-5 methyl of the thymine ring produces only a slight perturbation of the Tyr181 side-chain conformation.[12−17]

Dihydro-alkoxy-benzyl-oxopyrimidines (DABOs, **4**)[20−32] (Figure 1) belong to a NNRTI class reported in 1992.

Table 1. VALIDATE II and Autodock Predicted Activities for Compounds **9a**−**d**, **8d**, and MKC-442

	predicted activities	
compound	VALIDATE pIC_{50}[a]	Autodock pK_i[b]
9a	6.744	8.310
9b	7.033	8.527
9c	7.265	8.286
9d	8.305	8.654
8d	7.311	8.336
MKC-442	7.131[c]	6.910

[a] $pIC_{50} = -\log(IC_{50})$. IC_{50} values are expressed in μM. [b] $pK_i = -\log(K_i)$. K_i values are expressed in μM. [c] Fitted value from the VALIDATE II regression (see refs 26−28).

Since then, many structural modifications have been performed aimed at obtaining more potent derivatives (*S*-DABOs, **5**,[23,24] DATNOs, **6**[25]). Introduction of a 2,6-difluorophenylmethyl moiety as a C-6 substituent was one of the most favorable modifications, leading to compounds active in the low nanomolar range (difluoro-*S*-DABOs, F_2-*S*-DABOs, **7**, and conformationally constrained F_2-*S*-DABOs, **8**).[26−30]

Continuing this lead optimization, we describe the computer-aided design, synthesis, and biological evaluation of 2-alkylamino-6-[1-(2,6-difluorophenyl)alkyl]-3,4-dihydro-5-alkylpyrimidin-4(3*H*)-ones (difluoro-amino-DABOs, F_2-*NH*-DABOs) **9**, structurally related to the F_2-*S*-DABOs **7** and **8** in which the C-2-sulfur was replaced by nitrogen.

Molecular Design of F_2-*NH*-DABOs

Computational studies on the possible binding mode of F_2-*S*-DABO derivatives in the NNBP of HIV-1 RT, suggesting that the introduction of a further anchor point in the DABO molecular scaffold would lead to potentially more active derivatives, have recently been reported.[26,27] Replacement of the sulfur atom (placed in proximity of the RT backbone) with a nitrogen atom would lead to further, novel ligand/enzyme interactions. The new derivatives, named difluoro-amino-DABOs (F_2-*NH*-DABOs) in comparison to the previous F_2-*S*-DABOs contain a new anchor point, the C-2-NH group, which is at the same time both a donator and an acceptor of hydrogen bonds.

On the basis of these premises, molecular docking by means of the Autodock program was undertaken on four F_2-*NH*-DABOs (**9a**−**d**) structurally related to F_2-*S*-DABOs **8a**−**d**. For comparison purposes, the same docking procedure was carried out on the conformationally constrained F_2-*S*-DABO **8d**, and also on MKC-442 to assess the reliability of the docking procedure.

For docking studies the molecular structures of **9a**−**d** were directly built by modifying those of the previously reported computational studies on **8d**.[27] Compounds **8d**, **9c**, and **9d** were modeled in their *R* configuration.[28] The structures of **9a**−**d** were geometrically refined by simulated annealing dynamics and then were docked into the HIV-1 RT NNBP (see docking procedure in Experimental Section).

The docking studies on **9a**−**d** were in good agreement with the observation that introduction of two methyl groups at both C-5 and the methylene bridge between the pyrimidine and phenyl rings induces a conformation restriction of the active conformers.[27] In fact, the number of Autodock multi-member conformation clus-

Table 2. Anti-HIV-1 rRT, Anti-HIV-1, and Cytotoxicity of Compounds **8**, **9**[a]

	predicted values, μM		experimental values, μM			
compd	VALIDATE II IC_{50}	Autodock K_i	IC_{50}[b]	EC_{50}[c]	CC_{50}[d]	SI[e]
9a	0.180	0.005	0.070	0.09	>200	>2222
9b	0.093	0.003	0.030	0.02	>200	>10 000
9c	0.054	0.005	0.040	0.03	76	3500
9d	0.005	0.002	0.035	0.02	90	4500
8a[f]	ND[g]	ND	0.080	0.08	>200	>2500
8b[f]	ND	ND	0.080	0.08	>200	>2500
8c[f]	ND	ND	0.030	0.03	>200	>6666
8d[f]	0.049	0.005	0.005	0.006	>200	>33 333
MKC-442	0.074[h]	0.123	0.040	0.030	200	6666

[a] Data represent mean values of at least two separate experiments. [b] Compound dose required to inhibit the HIV-1 rRT activity by 50%. [c] Compound dose required to achieve 50% protection of MT4 cells from HIV-1 induced cytopathogenicity, as determined by the MTT method. [d] Compound dose required to reduce the viability of mock-infected cells by 50%, as determined by the MTT method. [e] Selectivity index, CC_{50}/EC_{50} ratio. [f] Ref 27. [g] ND, not determined. [h] Literature value[17] used for the formulation of the VALIDATE II model (see refs 33−35).

Table 3. Activity of **8d** and **9d** Against the Y181C HIV-1 Mutant Strain Compared to Those of Reference Drugs Nevirapine and Efavirenz

	EC_{50}, μM[a]		
compound	WT_{IIIB}	Y181C	(Y181C/WT_{IIIB})[b]
8d	0.015	0.20	(13)
9d	0.030	0.16	(5.3)
nevirapine	0.370	>30	(>81)
efavirenz	0.004	0.025	(6)

[a] Compound dose required to achieve 50% protection of MT4 cells from wild type and Y181C HIV-1 induced cytopathogenicity, as determined by the MTT method. [b] Fold resistance.

Table 4. Autodock Results

compound	number of distinct conformational clusters	number of multi-member conformational clusters	number of conformations in the first ranked cluster
8d	5	2	58
9a	22	10	38
9b	42	14	18
9c	18	8	38
9d	17	6	54
MKC-442	46	9	27

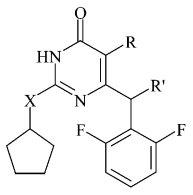

8a: X = S; R = R' = H;
8b: X = S; R = CH_3, R' = H;
8c: X = S; R = H, R' = CH_3;
8d: X = S; R = R' = CH_3

9a: X = NH; R = R' = H;
9b: X = NH; R = CH_3, R' = H;
9c: X = NH; R = H, R' = CH_3;
9d: X = NH; R = R' = CH_3.

Figure 2. Chemical structures of F_2-*S*-DABOs and F_2-*NH*-DABOs.

ters (Table 4 in Experimental Section) was found to be the lowest for **9d**, which is structurally related to the conformationally constrained F_2-*S*-DABO **8d**. The first-ranking conformational clusters were also the most populated; thus, they were used for the definition of the F_2-*NH*-DABO binding mode.

First-ranking docked conformations are reported in Figure 3. It can be seen that the binding modes proposed by Autodock for **9a**−**d** are fairly close to each other. Similarly, as previously reported, DABOs do not superimpose completely with MKC-442, reinforcing the differences in structure−activity relationships discussed between the two families.[29,30] F_2-*NH*-DABO binding conformations are characterized by a "propeller-like" disposition of the thymine/uracil and 2,6-difluorophenyl rings, with average τ_1 and τ_2 values of −62.5° and 91.5° (Figure 3). These values are in close agreement with those reported previously.[27]

The 2-amino-4(3*H*)-pyrimidinone NH−CH−NH−C═O moiety of each amino-DABO (Figure 4) is engaged in three hydrogen bonds, two with the C═O and one with the N−H function of Lys101. The 2,6-difluorophenyl ring contacts favorably the Tyr181 side chain (positive π-stacking interaction) and fits the aromatic-rich pocket of the NNBP formed by the side chains of Pro95, Tyr181, Tyr188, Phe227, Trp229, and Leu234. The cyclopentyl substituent fits into the Pro236 hairpin pocket.[16] Finally, the methylene and/or the C-5-methyl groups (when present) are positioned in a small hydrophobic cavity formed by the Val179 side chain and portions of other residues.

A hybrid QSAR/scoring function model (VALIDATE II),[33−35] specifically developed for studying the interaction of different NNRTIs within the NNBP and derived by a variation of the VALIDATE method,[36] was used to predict the biological activities of the F_2-*NH*-DABOs **9a**−**d**. pIC_{50} and pK_i values of **9a**−**d** and **8d**, predicted by VALIDATE II and by the internal scoring function of the Autodock program, respectively, are reported in Table 1.

Although belonging to a different type of measurements, the above values are in good agreement with each other, thus supporting the docking findings. This prompted us to initiate the synthesis and biological evaluation of the four F_2-*NH*-DABO prototypes **9a**−**d**.

Chemistry

The synthesis of **9a**−**d** was performed by heating the appropriate 5-alkyl-6-(2,6-difluorophenylalkyl)-3,4-dihydro-2-methylthiopyrimidin-4(3*H*)-one[26,27] with cyclopentylamine in a sealed tube at 170 °C for 8 h (Scheme 1). Nucleophilic displacement of the pyrimidinone C-2-methylthio group, exerted by the primary amine, afforded the required compounds.

Results and Discussion

The synthesis and biological properties of *S*-DABOs,[23,24] DATNOs,[25] and F_2-*S*-DABOs[26−30] were described in earlier publications beginning in 1992 and represent stepwise improvements of the DABOs family,[31,32] initially reported as new NNRTIs structurally related to HEPTs. In an attempt to develop novel DABOs with improved biological activity, molecular modeling studies were undertaken.

Docking studies of four F_2-*NH*-DABOs into the HIV-1 NNBP revealed that they could bind to the NNBP similarly to F_2-*S*-DABOs.[27] When compared to the structurally related HEPT-derivative MKC-442, F_2-*NH*-DABOs displayed a slightly different binding mode. A molecular inspection of F_2-*NH*-DABOs and MKC-442 X-ray[17] structures into the HIV-1 RT NNBP showed that they are not fully superimposable when their pyrimidine rings occupy the same NNBP space. In particular, the C-5-*iso*-propyl group of MKC-442, which

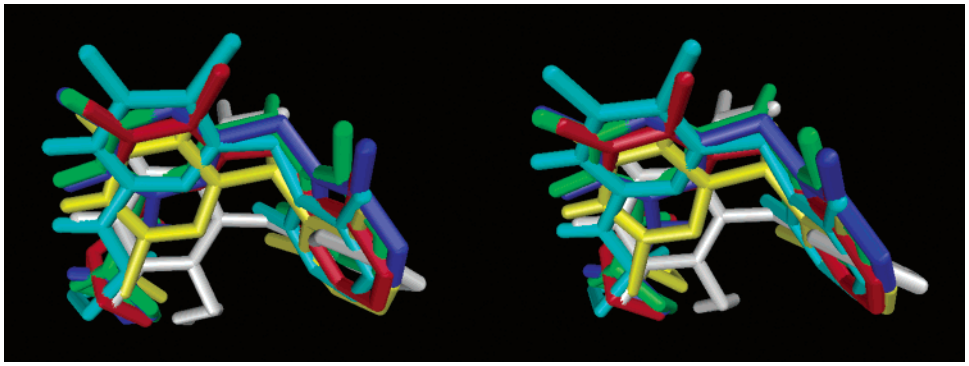

Figure 3. Stereoview superimposition of the docked **9a** (blue), **9b** (green), **9c** (red), and **9d** (cyan) with **8d** (yellow) and MKC-442 (white). Hydrogen atoms are not displayed for the sake of clarity.

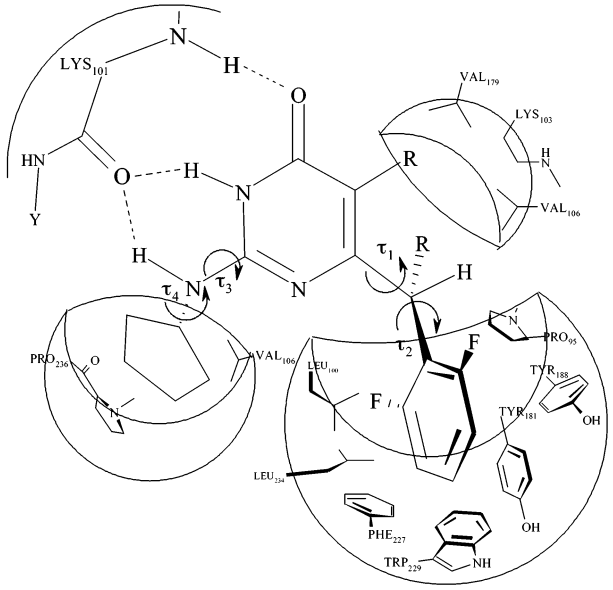

Figure 4. Scheme of the F_2-*NH*-DABOs/RT binding mode interactions.

Scheme 1

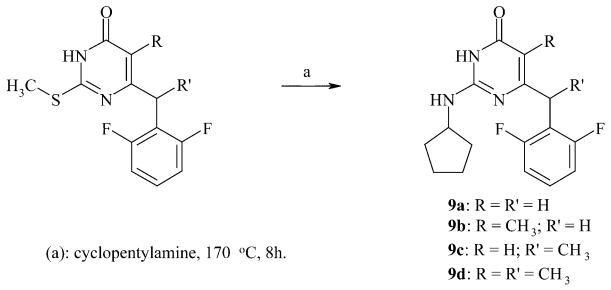

is responsible for the "trigger action", does not coincide with the C-5 position of compounds **9c** and **9d**. Moreover, the methylene linkages connecting the pyrimidinones to the phenyl rings lie in different positions (Figure 3).

Within the NNBP, F_2-*NH*-DABOs establish several ligand−receptor interactions. In particular, inspection of the **9d**/RT complex (Figures 4 and 5) shows (i) a hydrogen bond donated by the 3-NH function of the pyrimidine to the carbonyl oxygen of Lys101 (N−O distance = 2.726 Å); (ii) a hydrogen bond accepted by the C-4 carbonyl oxygen of the pyrimidine from the amide NH of Lys101 (O−N distance = 3.211 Å); (iii) a hydrogen bond donated by the C-2 NH group to the carbonyl oxygen of Lys101 (N−O distance = 2.779 Å); (iv) favorable steric interactions between the cyclopentyl moiety and the pyrrolidine ring of Pro236 and *iso*-propyl chain of Val106; (v) favorable steric interactions of the **9d** difluorophenyl ring with a hydrophobic pocket defined by the side-chains of Tyr188, Trp229, Phe227, Tyr181, Leu100, Pro95, and Leu234; (vi) favorable π-stacking between the electron-deficient difluorophenyl ring of F_2-*NH*-DABOs and the electron-rich benzene ring of Tyr188; (vii) favorable steric interactions of the C-5 and methylene linkage methyl groups with a hydrophobic pocket defined by the Val179, Lys103, and Val106 side-chains.

Docking results were confirmed by a quantitative prediction of anti-HIV-1 RT activity for the new F_2-*NH*-DABOs. Autodock calculated the K_i of the newly designed derivatives in the nanomolar range, and the VALIDATE II model predicted the corresponding IC_{50} values in the submicromolar range for **9a**−**c** and in the nanomolar range for **9d** (Table 1). To confirm such predicted, high inhibitory activities, F_2-*NH*-DABOs **9a**−**d** were synthesized and tested. The anti-HIV-1 activity and cytotoxicity of **9a**−**d** were evaluated both in MT-4 cells and in an enzyme assay using nevirapine and MKC-442 as reference compounds (Table 2).

Data in Table 2 suggest that the anti-HIV-1 activity profile of amino-DABOs **9a**−**d** is quite different from that of thio-DABOs **8a**−**d**. In fact, in the F_2-*S*-DABO series, introduction of a methyl substituent both at the C-6 methylene linkage and at the C-5 position of pyrimidine was crucial for the anti-HIV-1 activity in enzyme as well as in the cell-based assay.[27] On the contrary, in F_2-*NH*-DABOs the same double substitution results in no difference in potency. This finding could be explained by the presence, in **9a**−**d**, of a new anchor point represented by the C-2 NH group, that tightens binding of the inhibitors to the enzyme through a new hydrogen bond with the Lys101 main chain (Figure 5). In particular, this new **9d**/RT interaction seems to diminish the structural and biological role of the double C-5/benzylic methyl substitution (compare **8a** to **8d** and **9a** to **9d**), which in the thio-DABO series is responsible for both the selection of the constrained binding conformation of the ligand and the enhanced ligand/enzyme positive hydrophobic interactions. The increased number of hydrogen bonds between **9a**−**d** and the NNBP (Lys101−Lys103−Leu100 side) also reduces the biological effect of favorable π-stacking interactions between the DABO difluorophenyl moiety and NNBP (Tyr181−

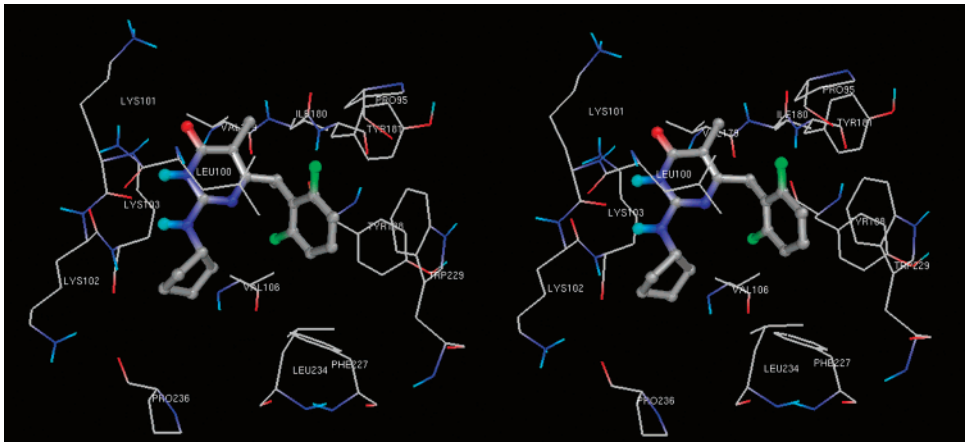

Figure 5. Docking results of **9d** into the NNBP. Only closely interacting residues are showed. Hydrogen atoms are not displayed for the sake of clarity.

Tyr188 side). As a result, **9d** could be expected to be less susceptible than **8d** to decreasing activity when tested against the Y181C mutated strain of HIV-1. Actually, when tested against the Y181C HIV-1 mutant, the F_2-*NH*-DABO **9d** was found to be only 5.3 times less active than in the HIV-1 wt assay (Table 3), whereas in the same assays F_2-*S*-DABO **8d** declined by a factor of 13 in anti-HIV-1 activity. This resistance profile of **9d** is slightly better than that of efavirenz (Table 3), the last FDA-approved NNRTI for AIDS therapy.

Conclusion

Novel DABOs derivatives **9a**−**d** (F_2-*NH*-DABOs) bearing a NH group at the C-2 pyrimidine position have been designed using computational methods. VALIDATE II and Autodock predicted activities of newly designed DABOs prompted their synthesis and biological evaluation. The experimental data confirmed the computational predictions for the new F_2-*NH*-DABOs: when tested against wild-type HIV-1, **9a**−**d** showed antiviral activities comparable or slightly lower than those of F_2-*S*-DABOs both in enzyme and cell-based assay. Interestingly, in comparison with *S*-DABOs, some enhancement of potency was achieved by testing amino-DABOs against the Y181C mutant strain. These results seem to be due to the introduction in amino-DABOs of a new anchor point (pyrimidine C-2 NH group), that could compensate for the incoming lack of positive hydrophobic ligand/NNBP interactions due to Tyr181 to Cys181 mutation through a new hydrogen bond with Lys101. Thus, the F_2-*NH*-DABOs can be promising novel DABO candidates for further synthesis, and biological and pharmacological studies aimed to evaluate their effectiveness as anti-AIDS agents active against both wild type and mutated strains of HIV-1.

Experimental Section

Chemistry. Melting points were determined on a Büchi 530 melting point apparatus and are uncorrected. Infrared (IR) spectra (KBr) were recorded on a Perkin-Elmer 297 instrument. ^{1}H NMR spectra were recorded at 200 MHz on a Bruker AC 200 spectrometer; chemical shifts are reported in δ (ppm) units relative to the internal reference tetramethylsilane (Me_4Si). All compounds were routinely checked by TLC and ^{1}H NMR. TLC was performed on aluminum-backed silica gel plates (Merck DC−Alufolien Kieselgel 60 F_{254}) with spots visualized by UV light. All solvents were reagent grade and, when necessary, were purified and dried by standard methods. Concentration of solutions after reactions and extractions involved the use of a rotary evaporator operating at a reduced pressure of ca. 20 Torr. Organic solutions were dried over anhydrous sodium sulfate. Analytical results are within ±0.40% of the theoretical values.

General Procedure for the Preparation of 5-Alkyl-2-cyclopentylamino-6-(2,6-difluorophenylalkyl)-3,4-dihydropyrimidin-4(3*H*)-ones 9a−d. Preparation of 2-Cyclopentylamino-6-(2,6-difluorophenylmethyl)-3,4dihydropyrimidin-4(3*H*)-one (9a). A mixture of 6-(2,6-difluorophenylmethyl)-3,4-dihydro-2-methylthiopyrimidin-4(3*H*)-one[26] (0.5 g, 1.86 mmol) and cyclopentylamine (5 mL) was heated in a sealed tube at 170 °C for 8 h. After cooling of sample, the crude residue was dissolved in ethyl acetate (50 mL), washed with water (50 mL), 0.5 N HCl (50 mL), and brine (50 mL), and then evaporated under reduced pressure and purified by column chromatography (silica gel/chloroform). Yield, 53%; oil. IR: 3280 (NH), 2920 (NH), 1640 (CO) cm^{-1}. ^{1}H NMR ($CDCl_3$): δ 1.26−1.59 (m, 8H, C-2,3,4,5 cyclopentane-H), 3.91 (s, 2H, CH_2), 4.10−4.13 (m, 1H, cyclopentane H-1), 5.32 (s, 1H, C-5 H), 6.44−6.48 (d, 1H, N*H*-cyclopentane, exchanged with D_2O), 6.68−6.92 (t, 2H, C-3,5 Ar−H), 7.17−7.28 (m, 1H, C-4 Ar−H), 11.11 (s, 1H, CONH, exchanged with D_2O). Anal. ($C_{16}H_{17}F_2N_3O$) C, H, N, F.

In a procedure analogous to the synthesis of **9a**, compounds **9b**−**d** were prepared from the appropriate 5-alkyl-6-(2,6-difluorophenylalkyl)-3,4-dihydro-2-methylthiopyrimidin-4(3*H*)-ones.[26,27]

2-Cyclopentylamino-6-(2,6-difluorophenylmethyl)-3,4-dihydro-5-methylpyrimidin-4(3*H*)-one (9b). Yield, 62%; mp 115−117 °C (*n*-hexane/cyclohexane). IR: 3290 (NH), 2940 (NH), 1635 (CO) cm^{-1}. ^{1}H NMR ($CDCl_3$): δ 1.28−1.60 (m, 8H, C-2,3,4,5 cyclopentane-H), 2.01 (s, 3H, CH_3), 3.90 (s, 2H, CH_2), 4.12−4.15 (m, 1H, cyclopentane H-1), 6.45−6.53 (d, 1H, N*H*-cyclopentane, exchanged with D_2O), 6.70−6.94 (t, 2H, C-3,5 Ar−H), 7.15−7.27 (m, 1H, C-4 Ar−H), 11.09 (s, 1H, CONH, exchanged with D_2O). Anal. ($C_{17}H_{19}F_2N_3O$) C, H, N, F.

2-Cyclopentylamino-6-[1-(2,6-difluorophenyl)ethyl]-3,4-dihydropyrimidin-4(3*H*)-one (9c). Yield, 60%; oil. IR: 3300 (NH), 2930 (NH), 1630 (CO) cm^{-1}. ^{1}H NMR ($CDCl_3$): δ 1.30−1.70 (m, 8H, C-2,3,4,5 cyclopentane-H), 1.58−1.64 (d, 3H, CHC*H*$_3$ overlapped signal), 3.95−4.03 (q, 1H, C*H*-CH_3) 4.21−4.32 (q, 1H, cyclopentane H-1), 5.51 (s, 1H, C-5 H), 6.37−6.40 (d, 1H, N*H*-cyclopentane, exchanged with D_2O), 6.79−6.87 (t, 2H, C-3,5 Ar−H), 7.12−7.19 (m, 1H, C-4 Ar−H), 11.22 (s, 1H, CONH, exchanged with D_2O). Anal. ($C_{17}H_{19}F_2N_3O$) C, H, N, F.

2-Cyclopentylamino-6-[1-(2,6-difluorophenyl)ethyl]-3,4-dihydro-5-methylpyrimi din-4(3*H*)-one (9d). Yield, 62%; oil. IR: 3290 (NH), 2940 (NH), 1640 (CO) cm^{-1}. ^{1}H NMR ($CDCl_3$): δ 1.26−1.72 (m, 8H, C-2,3,4,5 cyclopentane-H), 1.56−1.60 (d, 3H, CHC*H*$_3$ overlapped signal), 1.88 (s, 3H, C-5 CH_3), 4.08−4.21 (q, 1H, C*H*-CH_3) 4.45−4.56 (q, 1H, cyclopentane

H-1), 6.04−6.10 (d, 1H, N*H*-cyclopentane, exchanged with D_2O), 6.79−6.87 (t, 2H, C-3,5 Ar−H), 7.07−7.15 (m, 1H, C-4 Ar−H), 11.43 (s, 1H, CONH, exchanged with D_2O). Anal. ($C_{18}H_{21}F_2N_3O$) C, H, N, F.

Computational Studies. All molecular modeling calculations and manipulations were performed using the software packages Macromodel 7.1,[37] Autodock 3.0.5,[38] running on Silicon Graphics O2 R10000, IBM-compatible Intel Pentium IV 1.4 GHz and AMD Athlon 1.9 GHz workstations. For minimizations the all-atom Amber force field[39] was adopted as implemented in the Macromodel package.

The geometry of the RT NNBP was taken from the structure of the HIV-1 RT/MKC-442 complex filed in the Brookhaven Protein Data Bank[40] (entry code 1rt1). All the residues within 20 Å from any ligand's atom (MKC-442) were used to define the NNBP.

The structures of compounds **8d** and **9a**−**d** were directly built from those of previously reported computational studies on *S*-DABOs.[26,27] Compounds **8d**, **9c**, and **9d** were modeled in their *R* configurations.[28]

Starting conformations for the docking studies were obtained using molecular dynamics with simulated annealing as implemented in Macromodel version 7.1 and conducted as follows: **9a**−**d** were energy minimized to a low gradient. The nonbonded cutoff distances were set to 20 Å for both van der Waals and electrostatic interactions. An initial random velocity to all atoms corresponding to 300 K was applied. Three subsequent molecular dynamic runs were then performed. The first was carried out for 10 ps with a 1.5 fs time-step at a constant temperature of 300 K for equilibration purposes. The next molecular dynamic was carried out for 20 ps, during which the system is coupled to a 150 deg thermal bath with a time constant of 5 ps. The time constant represents approximately the half-life for equilibration with the bath; consequently, the second molecular dynamic command caused the molecule to slowly cool to approximately 150 K. The third and last dynamic cooled the molecule to 50 K over 20 ps. A final energy minimization was then carried out for 250 iterations using the conjugate gradient method. The minimizations and the molecular dynamics were performed in aqueous solution in all cases. The atom charges automatically assigned by the batchmin module were retained on **9a**−**d** for the docking calculations.

For the docking procedure, the program Autodock was used to explore the binding conformation of **9a**−**d**. For the docking a grid spacing of 0.375 Å and 60 × 80 × 60 number of points were used. The grid was centered on the mass center of the experimental bound MKC-442 coordinates. The GA-LS method was adopted using the default settings. Amber united atoms were assigned to the protein using the program ADT (AutoDock Tools). Autodock generated 100 possible binding conformations for **9a**−**d**.

To validate the use of the Autodock program, the docking studies were performed on the reference compounds MKC-442 and for comparison purposes also on the previously reported F_2-*S*-DABO **8d**. Autodock successfully reproduced the experimental binding conformations of the reference drug with acceptable root-mean-square deviation (RMSD) of atom coordinates.

The results of the Autodock runs which were clustered using an RMSD tolerance of 0.5 Å are summarized in Table 4.

A VALIDATE II model specifically for the NNRTIs was used to estimate the binding conformation of the docking studies analogously as previously reported.[33]

Antiviral. Assay Procedures. Compounds. Compounds were solubilized in DMSO at 200 mM and then diluted into culture medium.

Cells and Viruses. MT-4, C8166, H9/III_B, and CEM cells were grown at 37 °C in a 5% CO_2 atmosphere in RPMI 1640 medium, supplemented with 10% fetal calf serum (FCS), 100 IU/mL penicillin G, and 100 μg/mL streptomycin. Cell cultures were checked periodically for the absence of mycoplasma contamination with a MycoTect Kit (Gibco). Human immunodeficiency viruses type-1 (HIV-1, III_B strain) and type-2 (HIV-2 ROD strain, kindly provided by Dr. L. Montagnier, Paris) were obtained from supernatants of persistently infected H9/III_B and CEM cells, respectively. HIV-1 and HIV-2 stock solutions had titers of 4.5×10^6 and 1.4×10^5 50% cell culture infectious dose ($CCID_{50}$)/mL, respectively.

HIV Titration. Titration of HIV was performed in C8166 cells by the standard limiting dilution method (dilution 1:2, four replica wells per dilution) in 96-well plates. The infectious virus titer was determined by light microscope scoring of cytopathicity after 4 days of incubation and the virus titers were expressed as $CCID_{50}$/mL.

Anti-HIV Assays. Activity of the compounds against HIV-1 and HIV-2 multiplication in acutely infected cells was based on the inhibition of virus-induced cytopathicity in MT-4 and C8166 cells, respectively. Briefly, 50 μL of culture medium containing 1×10^4 cells were added to each well of flat-bottom microtiter trays containing 50 μL of culture medium with or without various concentrations of the test compounds. Then, 20 μL of an HIV suspension containing 100 (HIV-1) or 1000 (HIV-2) $CCID_{50}$ (50% cell culture infective dose) were added. After a 4-day incubation (5 days for HIV-2) at 37 °C, the number of viable cells was determined by the 3-(4,5-dimethylthiazol-1-yl)-2,5-diphenyltetrazolium bromide (MTT) method.[41] Cytotoxicity of the compounds was evaluated in parallel with their antiviral activity. It was based on the viability of mock-infected cells, as monitored by the MTT method.

RT Assays. Assays were performed as previously described.[42] Briefly, purified rRT was assayed for its RNA-dependent polymerase-associated activity in a 50 μL volume containing: 50 mM Tris-HCl (pH 7.8), 80 mM KCl, 6 mM $MgCl_2$, 1 mM DTT, 0.1 mg mL^{-1} BSA, 0.5 OD_{260} unit mL^{-1} template/primer [poly(rC)-oligo$(dG)_{12-18}$] and 10 mM [^{3}H]dGTP (1 Ci $mmol^{-1}$). After incubation for 30 min at 37 °C, the samples were spotted on glass fiber filters (Whatman GF/A), and the acid-insoluble radioactivity was determined.

Acknowledgment. We would like to thank Prof. Garland R. Marshall of the Molecular Biophysics Center for Computational Biology at Washington University Medical School − St. Louis (MO), for many insightful discussions and critical reading of this manuscript. This work was supported by Italian Ministero della Sanità − Istituto Superiore di Sanità − IV Programma nazionale di ricerca sull' AIDS 2001 (Grant nos. 40D.08 and 9403-59), Italian MURST (40% funds) and Regione Autonoma Sardegna (Assessorato Sanità).

References

(1) Yarchoan, R.; Mitsuya, H.; Thomas, R. V.; Pluda, J. M.; Hartman, N. R.; Perno, C. F.; Marczyk, K. S.; Allain, J. P.; Johns, D. G.; Broder, S. In vivo activity against HIV and favorable toxicity profile of 2′,3′-dideoxyinosine. *Science* **1989**, *245*, 412−415.
(2) Richman, D. D. Resistance of clinical isolates of human immunodeficiency virus to antiretroviral agents. *Antimicrob. Agents Chemother.* **1993**, *37*, 1207−1213.
(3) Artico, M. Nonnucleoside anti-HIV-1 reverse transcriptase inhibitors (NNRTIs): a chemical survey from lead compounds to selected drugs for clinical trials. *Farmaco* **1996**, *51*, 305−331.
(4) Pedersen, O. S.; Pedersen, E. B. Nonnucleoside reverse transcriptase inhibitors: the NNRTI boom. *Antivir. Chem. Chemother.* **1999**, *10*, 285−314.
(5) Hajòs, G.; Riedl, Z.; Molnàr, J.; Szabo, D. Nonnucleoside reverse transcriptase inhibitors. *Drug Future* **2000**, *25*, 47−62.
(6) De Clercq, E. Toward improved anti-HIV chemotherapy: therapeutic strategies for intervention with HIV infections. *J. Med. Chem.* **1995**, *38*, 2491−2517.
(7) De Clercq, E. Antiviral therapy for human immunodeficiency virus infections. *Clin. Microbiol. Rev.* **1995**, *8*, 200−239.
(8) Campiani, G.; Ramunno, A.; Maga, G.; Nacci, V.; Fattorusso, C.; Catalanotti, B.; Morelli, E.; Novellino, E. Non-Nucleoside HIV-1 Reverse Transcriptase (RT) Inhibitors: Past, Present, and Future Perspectives. *Curr. Pharm. Des.* **2002**, *8*, 615−657.
(9) De Clercq, E.; Balzarini, J. Knocking out human immunodeficiency virus through non-nucleoside reverse transcriptase inhibitors used as single agents or in combinations: a paradigm for the cure of AIDS? *Farmaco* **1995**, *50*, 735−747.

(10) De Clercq, E. The role of non-nucleoside reverse transcriptase inhibitors (NNRTIs) in the therapy of HIV-1 infection. *Antiviral Res.* **1998**, *38*, 153−179.
(11) De Clercq, E. Perspectives of non-nucleoside reverse transcriptase inhibitors (NNRTIs) in the therapy of HIV-1 infection. *Farmaco* **1999**, *54*, 26−45.
(12) Ren, J.; Esnouf, R.; Garman, E.; Somers, D.; Ross, C.; Kirby, I.; Keeling, J.; Darby, G.; Jones, Y.; Stuart, D.; Stammers, D. High-Resolution Structures of HIV-1 RT from Four RT-Inhibitor Complexes. *Nat. Struct. Biol.* **1995**, *2*, 293−302.
(13) Ding, J.; Das, K.; Tantillo, C.; Zhang, W.; Clark, A. D., Jr; Jessen, S.; Lu, X.; Hsiou, Y.; Jacobo-Molina, A.; Andries, K.; Pauwels, R.; Moereels, H.; Koymans, L.; Janseen, P. A.; Smith, R. H., Jr.; Kroeger Koepke, M.; Michejda, C. J.; Hughes, S. H.; Arnold, E. Structure of HIV-1 Reverse Transcriptase in a Complex with the Non-Nucleoside Inhibitor α-APA R 95845 at 2.8 Å Resolution. *Structure* **1995**, *3*, 365−379.
(14) Ding, J.; Das, K.; Moereels, H.; Koymans, L.; Andries, K.; Janssen, P. A.; Hughes, S. H.; Arnold, E. Structure of HIV-1 RT/TIBO R 86183 complex reveals similarity in the binding of diverse nonnucleoside inhibitors. *Nat. Struct. Biol.* **1995**, *2*, 407−415.
(15) Ren, J.; Esnouf, R.; Hopkins, A.; Ross, C.; Jones, Y.; Stammers, D.; Stuart, D. The structure of HIV-1 reverse transcriptase complexed with 9-chloro- TIBO: lessons for inhibitor design. *Structure* **1995**, *3*, 915−926.
(16) Esnouf, R. M.; Ren, J.; Hopkins, A. L.; Ross, C. K.; Jones, E. Y.; Stammers, D. K.; Stuart, D. I. Unique features in the structure of the complex between HIV-1 reverse transcriptase and the bis-(heteroaryl)piperazine (BHAP) U-90152 explain resistance mutations for this nonnucleoside inhibitor. *Proc. Natl. Acad. Sci. U.S.A.* **1997**, *94*, 3984−3989.
(17) Hopkins, A. L.; Ren, J.; Esnouf, R. M.; Willcox, B. E.; Jones, E. Y.; Ross, C.; Miyasaka, T.; Walker, R. T.; Tanaka, H.; Stammers, D. K.; Stuart, D. I. Complexes of HIV-1 reverse transcriptase with inhibitors of the HEPT series reveal conformational changes relevant to the design of potent non-nucleoside inhibitors. *J. Med. Chem.* **1996**, *39*, 1589−1600.
(18) Esnouf, R. M.; Stuart, D. I.; De Clercq, E.; Schwartz, E.; Balzarini, J. Models which explain the inhibition of reverse transcriptase by HIV-1- specific (thio)carboxanilide derivatives. *Biochem. Biophys. Res. Commun.* **1997**, *234*, 458−464.
(19) Baba, M.; Shigeta, S.; Yuasa, S.; Takashima, H.; Sekiya, K.; Ubasawa, M.; Tanaka, H.; Miyasaka, T.; Walker, R. T.; De Clercq, E. Preclinical evaluation of MKC-442, a highly potent and specific inhibitor of human immunodeficiency virus type 1 in vitro. *Antimicrob. Agents Chemother.* **1994**, *38*, 688−692.
(20) Tramontano, E.; Marongiu, M. E.; de Montis, A.; Loi, A. G.; Artico, M.; Massa, S.; Mai, A.; la Colla, P. Characterization of the anti-HIV-1 activity of 3,4-dihydro-2-alkoxy-6-benzyl-4-oxopyrimidines (DABOs), new non-nucleoside reverse transcriptase inhibitors. *Microbiologica* **1994**, *17*, 269−279.
(21) Massa, S.; Mai, A.; Artico, M.; Sbardella, G.; Tramontano, E.; Loi, A. G.; Scano, P.; La Colla, P. Synthesis and antiviral activity of new 3,4-dihydro-2-alkoxy-6-benzyl-4-oxopyrimidines (DABOs), specific inhibitors of human immunodeficiency virus Type-1. *Antiviral Chem. Chemother.* **1996**, *6*, 1−8.
(22) Artico, M.; Massa, S.; Mai, A.; Marongiu, M. E.; Piras, G.; Tramontano, E.; La Colla, P. 3,4-Dihydro-2-alkoxy-6-benzyl-4-oxopyrimidines (DABOs): a New Class of Specific Inhibitors of Human Immunodeficiency Virus Type 1. *Antiviral Chem. Chemother.* **1993**, *4*, 361−368.
(23) Ettorre, A.; Mai, A.; Artico, M.; Massa, S.; De Montis, A.; La Colla, P. 6-(3-Methylbenzyl)-2-(2-methylpropyl)thio-4(3*H*)-pyrimidinone (DABO 622). *Acta Crystallogr.* **1996**, *C52*, 2115−2117.
(24) Mai, A.; Artico, M.; Sbardella, G.; Massa, S.; Loi, A. G.; Tramontano, E.; Scano, P.; La Colla, P. Synthesis and anti-HIV-1 activity of thio analogues of dihydroalkoxybenzyloxopyrimidines. *J. Med. Chem.* **1995**, *38*, 3258−3263.
(25) Mai, A.; Artico, M.; Sbardella, G.; Quartarone, S.; Massa, S.; Loi, A. G.; De Montis, A.; Scintu, F.; Putzolu, M.; La Colla, P. Dihydro(alkylthio)(naphthylmethyl)oxopyrimidines: novel non-nucleoside reverse transcriptase inhibitors of the S-DABO series. *J. Med. Chem.* **1997**, *40*, 1447−1454.
(26) Mai, A.; Artico, M.; Sbardella, G.; Massa, S.; Novellino, E.; Greco, G.; Loi, A. G.; Tramontano, E.; Marongiu, M. E.; La Colla, P. 5-Alkyl-2-(alkylthio)-6-(2,6-dihalophenylmethyl)-3,4-dihydropyrimidin-4(3*H*)-ones: novel potent and selective dihydro-alkoxybenzyl-oxopyrimidine derivatives. *J. Med. Chem.* **1999**, *42*, 619−627.
(27) Mai, A.; Sbardella, G.; Artico, M.; Ragno, R.; Massa, S.; Novellino, E.; Greco, G.; Lavecchia, A.; Musiu, C.; La Colla, M.; Murgioni, C.; La Colla, P.; Loddo, R. Structure-based design, synthesis, and biological evaluation of conformationally restricted novel 2-alkylthio-6-[1-(2,6-difluorophenyl)alkyl]-3,4-dihydro-5-alkylpyrimidin-4(3*H*)-ones as non-nucleoside inhibitors of HIV-1 reverse transcriptase. *J. Med. Chem.* **2001**, *44*, 2544−2554.
(28) Quaglia, M.; Mai, A.; Sbardella, G.; Artico, M.; Ragno, R.; Massa, S.; del Piano, D.; Setzu, G.; Doratiotto, S.; Cotichini, V. Chiral resolution and molecular modeling investigation of rac-2-cyclopentylthio-6-[1-(2,6-difluorophenyl)ethyl]-3,4-dihydro-5- methylpyrimidin-4(3*H*)-one (MC-1047), a potent anti-HIV-1 reverse transcriptase agent of the DABO class. *Chirality* **2001**, *13*, 75−80.
(29) Sbardella, G.; Mai, A.; Artico, M.; Chimenti, P.; Maasa, S.; Loddo, R.; Marongiu, M. E.; La Colla, P.; and Pani, A. Structure−activity relationship studies on new DABOs: effect of substitutions at pyrimidine C-5 and C-6 positions on anti-HIV-1 activity. *Antiviral Chem. Chemother.* **2001**, *12*, 37−50.
(30) Artico, M.; Mai, A.; Sbardella, G.; Massa S.; La Colla, P. Does the 2-Methylthiomethyl Substituent Really Confer High Anti-HIV-1 Activity to S-DABOs? *Med. Chem. Res.* **2000**, *10*, 30−39.
(31) Marongiu, M. E.; Pani, A.; Musiu, C.; La Colla, P.; Mai, A.; Sbardella, G.; Massa, S.; Artico, M. 3,4-Dihydro-2-alkoxy-6-benzyl-oxopyrimidines (DABOs): Development of a potent class of non-nucleoside reverse transcriptase inhibitors. *Recent Res. Dev. Med. Chem.* **2002**, *1*, 65−92.
(32) Artico, M. Selected non-nucleoside reverse transcriptase inhibitors (NNRTIs): the DABOs family. *Drug. Future* **2002**, *27*, 159−175.
(33) Silvestri, R.; Artico, M.; De Martino, G.; Ragno, R.; Massa, S.; Loddo, R.; Murgioni, C.; Loi, A. G.; La Colla, P.; Pani, A. Synthesis, biological evaluation, and binding mode of novel 1-[2-(diarylmethoxy)ethyl]-2-methyl-5-nitroimidazoles targeted at the HIV-1 reverse transcriptase. *J. Med. Chem.* **2002**, *45*, 1567−1576.
(34) Ragno, R.; Artico, M.; Marshall, G. R. A predictive model for HIV non-nucleoside reverse transcriptase inhibitors. *XVIth International Symposium on Medicinal Chemistry*, Bologna, Italy, September 18−22, 2000. PC148.
(35) Manuscript in preparation. Briefly, a quantitative hybrid QSAR/scoring function model was obtained using 20 HIV-1 RT/inhibitor complexes 1bqm, 1c0t, 1c0u, 1dtq, 1dtt, 1eet, 1fk9, 1hni, 1hnv, 1klm, 1rev, 1rt1, 1rt2, 1rt3, 1rt4, 1rt5, 1rt6, 1rt7, 1vrt, 1vru, and 12 selected parameter/scores yielding to $r^2 = 0.88$, $q^2_{L5O} = 0.72$, $SDEP_{L5O} = 0.49$ using three principal pls components.
(36) Head, R. D.; Smythe, M. L.; Oprea, T. I.; Waller, C. L.; Green, S. M.; Marshall, G. R. VALIDATE−a new method for the receptor-based prediction of binding affinity of novel ligands. *J. Am. Chem. Soc.* **1996**, *118*, 3959−3969.
(37) Mohamadi, F.; Richards, N. G. J.; Guida, W. C.; Liskamp, R.; Lipton, M.; Caufield, C.; Chang, G.; Hendrickson, T.; Still, W. C. MacroModel−An Integrated Software System for Modeling Organic and Bioorganic Molecules Using Molecular Mechanics. *J. Comput. Chem.* **1990**, *11*, 440−467.
(38) Goodsell, D. S.; Morris, G. M.; Olson, A. J. Automated docking of flexible ligands: applications of AutoDock. *J. Mol. Recognit.* **1996**, *9*, 1−5.
(39) Pearlman, D. A.; Case, D. A.; Caldwell, J. W.; Ross, W. S.; Cheatham, T. E., I.; Debolt, S.; Ferguson, D. M.; Seibel, G. L.; Kollman, P. A. AMBER, a Package of Computer Programs for Applying Molecular Mechanics, Normal-Mode Analysis, Molecular Dynamics and Free Energy Calculations to Simulate the Structural and Energetic Properties of Molecules. *Comput. Phys. Commun.* **1995**, *91*, 1−41.
(40) Berman, H. M.; Westbrook, J.; Feng, Z.; Gilliland, G.; Bhat, T. N.; Weissig, H.; Shindyalov, I. N.; Bourne, P. E. The Protein Data Bank. *Nucleic Acids Res.* **2000**, *28*, 235−242.
(41) Pauwels, R.; Balzarini, J.; Baba, M.; Snoeck, R.; Schols, D.; Herdewijn, P.; Desmyter, J.; De Clercq, E. Rapid and automated tetrazolium-based colorimetric assay for the detection of anti-HIV compounds. *J. Virol. Methods* **1988**, *20*, 309−321.
(42) Tramontano, E.; Cheng, Y. C. HIV-1 reverse transcriptase inhibition by a dipyridodiazepinone derivative: BI-RG-587. *Biochem. Pharmacol.* **1992**, *43*, 1371−1376.

JM0309856